

one estimates wave speed down to some first set of strong reflectors, images those reflectors sufficiently accurately and then proceeds with velocity analysis down to the next set of reflectors, recursively moving progressively deeper into the medium. This topic will not be addressed here. However, see Meng [1998] for an extensive survey of velocity analysis techniques.

On the other hand, it is important to note that the medium can be thought of as having a range of characteristic lengths associated with its variation. We are finding an approximate solution to the inverse problem by using a background wave speed with which to propagate the data back into the medium. The length scale of that background should be one of the L 's satisfying our high frequency criterion, above. Using that background wave speed, we then detect the reflectors in the earth—the interfaces across which the medium varies rapidly enough to produce reflection responses at the scale of the wavelengths in the seismic experiment.

Actually, in practice, we cheat a little on this description. Once a reflector is identified, we allow for refractions across that interface when imaging deeper reflectors in the earth. That is, we allow for rapid variation in the background wave speed above the reflector of interest; it is only in the neighborhood of the *current* target reflector that we require smoothness of the background wave speed.

Of course, there are the intermediate length scales of the medium, neither long enough to satisfy the asymptotic criterion above, nor short enough to produce reflections for the given bandwidth. They are not well treated. Nonetheless, the method works reasonably well in producing images, although a rigorous mathematical theory would require a clear separation of scales relative to the wavelength.

Outline

The next section is largely based on Chapter 5 of Bleistein et al. [1998], which is a set of lecture notes that is moving towards publication as a textbook. It describes the basic inversion theory with one modernization from the lecture notes. In those notes, the Born approximation is used to provide the forward model from which the inversion result is deduced. The Born approximation is, essentially, a perturbation theory result, requiring small changes in medium parameters throughout the earth model. In the more recent derivation, the Kirchhoff approximation for the response from a single reflector is used. For the Kirchhoff approximation, the change in medium parameters across the given reflector need not be small. On the other hand, it is necessary to assume linearity in order to apply this one formula to the entire data set. Of course, linearization takes us back to the Born approximation. The only real advantage that we gain, here, is that we can now interpret the peak amplitude of an image in terms of the geometrical optics reflection coefficient, directly from the derivation. Previously, that required a separate analysis to see how the Born-based inversion formula treated Kirchhoff approximate data. In fact, the derived inversion formulas are identical. Hence, it should be no surprise that this latter test led to exactly the same interpretation of the peak amplitude as is directly determined

from the Kirchhoff-based derivation. Thus, while the Born approximation predicts an amplitude that is linear in the medium perturbations, the ultimate interpretation from the analysis of Kirchhoff data is that the output is linear in the geometrical optics reflection coefficient at a distinguished angle of incidence. This reflection coefficient is, itself, a *nonlinear* function of the medium parameter perturbations. Furthermore, the theory shows that distinguished specular angle can also be determined.

The final section of these notes addresses a relatively new idea that we call *Kirchhoff data mapping*. There are many preprocessing steps in the analysis of data sets designed to reduce the amount of data or simplify the source/receiver configuration of the seismic experiment. (Think of inverting data gathered on a mountainside, for example; 'much nicer to have data on a flat datum surface.) Some of these processes can be viewed as mapping the data from an input source/receiver configuration to an output source receiver configuration in a model consistent manner, using large length scale (with respect to the wave length) background earth models in the input and output configurations. It is possible to set down a platform for all of these problems. This platform then becomes a point of departure for specific implementations; the simplest of these is mapping data collected a fixed separation between source and receiver (common offset data) and mapping it to equivalent data with coincident source and receiver (zero offset data). It turns out that the spatial extent of the operator that achieves this mapping is less than the offset length, not very large compared to the length of a survey. The mapped zero offset data can then be inverted to produce a reflector map with faster and cheaper methods than are available for the finite offset data.

INVERSION OF KIRCHHOFF MODEL DATA FOR REFLECTION FROM A SINGLE REFLECTOR

The inverse scattering theory starts from a solution to the forward scattering problem. As noted earlier, this theory originally used the Born approximation to obtain that forward model data. It then requires further analysis to demonstrate that the output, either from ray theoretic or from Kirchhoff approximate reflection response data, is linear in the geometrical optics reflection coefficient. Here, we present a derivation of the inversion operator based on a Kirchhoff approximate forward model, thereby avoiding some of the linearity constraints of the Born approximation.

The derivation starts with the Kirchhoff approximation for the upward scattered wave from a single reflector. This representation can be found in many sources; we use equation (5.3.1) in Bleistein, et al [1998b].

$$u(\boldsymbol{\xi}, \omega) \sim i\omega F(\omega) \int_{S_R} a(\mathbf{x}, \boldsymbol{\xi}) \cdot \hat{\mathbf{n}}_R \cdot \nabla_x \tau(\mathbf{x}, \boldsymbol{\xi}) R(\mathbf{x}, \mathbf{x}_s) e^{i\omega\tau(\mathbf{x}, \boldsymbol{\xi})} dS_R. \quad (10)$$

In this equation, \mathbf{x} is a function of the surface parameters, say, (σ_1, σ_2) . The two component vector, $\boldsymbol{\xi}$, is used to parameterize the source and receiver locations, $\mathbf{x}_s(\boldsymbol{\xi})$ and $\mathbf{x}_g(\boldsymbol{\xi})$, respectively, and ω denotes the frequency of the output wave. The upward

unit normal to the reflecting surface, S_R is denoted by $\hat{\mathbf{n}}_R$. The phase and amplitude are given by

$$\tau(\mathbf{x}, \boldsymbol{\xi}) = \tau(\mathbf{x}, \mathbf{x}_s(\boldsymbol{\xi})) + \tau(\mathbf{x}, \mathbf{x}_g(\boldsymbol{\xi})) = \tau_s + \tau_g; \quad (11)$$

$$a(\mathbf{x}, \boldsymbol{\xi}) = A(\mathbf{x}, \mathbf{x}_s(\boldsymbol{\xi})) \cdot A(\mathbf{x}, \mathbf{x}_g(\boldsymbol{\xi})),$$

with the separate travel times and phases being solutions of appropriate eikonal and transport equations, respectively, with initial point, \mathbf{x}_s or \mathbf{x}_g , and final point, \mathbf{x} . We choose not to be more specific here, allowing for different propagation speeds in the eikonal equations (mode conversion) and transport equations appropriate to the degree of generality of the propagation model under consideration. The amplitudes can also include products of transmission coefficients arising from interfaces above the surface, S_R .

The function, $F(\omega)$ represents the detected source signature. We assume that our sources are all bandlimited delta functions with peak value at $t = 0$. Below, we will replace $F(\omega)$ by one and think of our inversion as being an approximation that leads to the “most singular part” of the solution of the inverse problem—that is, for the reflector surface as opposed to the slow medium parameter changes in the earth—and whatever medium parameter information we can glean from the result.

The two parameter description of source and receiver location allows us to subsume many realistic source/receiver configurations into this one representation. For example, consider the problem of a single source and an areal array of receivers over the plane, $z = 0$. For this case,

$$\mathbf{x}_s = \text{constant vector} = \mathbf{x}_0, \quad \mathbf{x}_g = (\xi_1, \xi_2, 0).$$

This is called a common shot experiment. As a second example consider a survey in which sources and receivers are kept at a fixed distance apart and moved on parallel lines. In this case,

$$\mathbf{x}_s = (\xi_1 - h, \xi_2, 0), \quad \mathbf{x}_g = (\xi_1 + h, \xi_2, 0).$$

This is called a common offset experiment. A third choice might be to place the source and receive in a line, then move along the line to repeat the experiment, but then repeat the entire ensemble on parallel lines. Clearly, this would be a practical experiment over water, where the receivers would be towed behind a boat on a cable with a source set off periodically. However, the same experiment could be carried out on land, with receivers on both sides of the source in each experiment. This experiment cannot be described as above, but has the form

$$\mathbf{x}_s = (\eta, \xi_2, 0), \quad (\eta + \xi_1, \xi_2, 0).$$

However, this ensemble of experiments has redundant data when we know a background wavespeed to use in our inversion. In fact, the previous data set can be extracted as a subset of this data set. The redundancy here leads to *multiple* solutions

of the inverse problem—for example, one for each common offset data subset. Those multiple solutions can be used for velocity analysis to determine that background wavespeed before inversion and to obtain multiple estimates of specular reflection coefficient at different incidence angles after inversion. For the latter, it is this multiplicity of specular incidence angles associated with the different inversions that will allow the unraveling of the reflection coefficient to actually determine the changes in medium parameters themselves across the reflector.

It should be noted that, except for the obliquity factor, $\hat{\mathbf{n}}_R \cdot \nabla_x \tau(\mathbf{x}, \boldsymbol{\xi})$, and the reflection coefficient, $R(\mathbf{x}, \mathbf{x}_s)$, the elements of the integrand are defined globally in \mathbf{x} and not just on the reflecting surface. That restricted dependence will be isolated further, to R , alone, in order to derive an inversion formula. Thus, what is needed is an approximation of the factor, $\hat{\mathbf{n}}_R \cdot \nabla_x \tau(\mathbf{x}, \boldsymbol{\xi})$ that is independent of surface information; more specifically, it is necessary to eliminate the dependence on $\hat{\mathbf{n}}_R$. The right choice here is the stationary value of this factor at the stationary point(s) of the original surface integral, (10),

$$\hat{\mathbf{n}}_R \cdot \nabla_x \tau(\mathbf{x}, \boldsymbol{\xi}) = -|\nabla_x \tau(\mathbf{x}, \boldsymbol{\xi})|. \quad (12)$$

In more detail, we find the stationary point(s) by setting the derivative of the phase with respect to the parameters, σ_1 and σ_2 equal to zero. This leads to the interpretation that the tangential components of the gradients of τ_s and τ_g must be equal and opposite in direction; this is Snell’s law. Then, (12) follows. We proceed in the discussion here as if there is one source/receiver pair associated with each \mathbf{x} in the subsurface, making for distinct “stationary triples”. On the one hand, this restricts our analysis to cases in which there is no “multi-pathing”—that is no caustics of the rays—between \mathbf{x} and \mathbf{x}_s or \mathbf{x}_g . However, it does allow that more than one specular point on the reflector might be associated with a particular $\boldsymbol{\xi}$ —a particular source/receiver pair—on the upper surface, as in Figure 1. To include multi-pathing, at the very least, we would have to modify the Green’s function amplitudes in equation (1) to account for phase shifts when the geometrical optics rays pass through caustics.

The right side of (12) is independent of the coordinates of the reflecting surface, which was our objective in making this approximation; we substitute this result into (10). This is consistent with the intent of deriving an inversion for the reflectivity function, only. It acknowledges that high frequency modeling and inversion uses reflection data to detect reflecting surfaces. With this approximation, (10) is rewritten as

$$u(\boldsymbol{\xi}, \omega) = -i\omega F(\omega) \int_{S_R} a(\mathbf{x}, \boldsymbol{\xi}) |\nabla_x \tau(\mathbf{x}, \boldsymbol{\xi})| R(\mathbf{x}, \mathbf{x}_s) \cdot e^{i\omega\tau(\mathbf{x}, \boldsymbol{\xi})} dS_R. \quad (13)$$

The next goal is to rewrite the integral in (13) as a volume integral by introducing the *singular function of the reflecting surface*, $\delta(n_R)$, where n_R measures normal distance from any point on the reflector. In Figure 3, we depict a bandlimited version of the singular function. The function, $\delta_B(\phi)$, introduced in the introduction is merely a scaled version of the singular function of a *curve* in two dimensions.

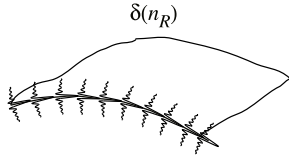


FIG. 3. The (bandlimited) singular function of a surface. The singular function is a delta function of a single argument that is zero on the surface.

The new representation becomes

$$u(\boldsymbol{\xi}, \omega) \sim -i\omega F(\omega) \int a(\mathbf{x}, \boldsymbol{\xi}) |\nabla_x \tau(\mathbf{x}, \boldsymbol{\xi})| \cdot R(\mathbf{x}, \mathbf{x}_s) \cdot \delta(n_R) e^{i\omega\tau(\mathbf{x}, \boldsymbol{\xi})} d^3x \quad (14)$$

Here, $dS_R dn_R = d^3x$. At worst, a reasonable continuation of the reflection coefficient off the reflecting surface must be introduced in this equation. Of course, that continuation need only correspond to the true R on the support of the singular function, that is, on the reflector. Even for bandlimited delta functions, this is easy to achieve.

Just as the normal derivative of the travel time has been replaced by its stationary value, the reflection coefficient is replaced by its stationary value, as well. Then, the product, $R\delta$, appearing in this equation is just the *reflectivity function*, $\beta(\mathbf{x})$, of the Bleistein/Cohen inversion theory [Bleistein, et al, 1998b, eq. 5.1.21]. In this case, (14) can be rewritten as

$$u(\boldsymbol{\xi}, \omega) \sim -i\omega F(\omega) \int a(\mathbf{x}, \boldsymbol{\xi}) |\nabla_x \tau(\mathbf{x}, \boldsymbol{\xi})| \beta(\mathbf{x}) e^{i\omega\tau(\mathbf{x}, \boldsymbol{\xi})} d^3x \quad (15)$$

This can be viewed as an integral equation for β , given the observed data, $u(\boldsymbol{\xi}, \omega)$. It has exactly the same structure as the integral equation for velocity perturbation in Chapter 5 of Bleistein, et al. [1998]. We will therefore follow the same procedure as in that chapter to invert this integral equation. What we are really doing is finding the *pseudo-inverse* for the operator, \mathcal{L} operating on β on the right side of this equation. That is, we are determining $[\mathcal{L}^* \mathcal{L}]^{-1} \mathcal{L}^*$. However, our approach will be more intuitive, avoiding a background in pseudo-differential operator theory to follow the derivation.

The structure of the inversion operator can be gleaned from kernels of operators for simpler problems. For example, we have derived inversion formulas for the case of constant background wavespeed by Fourier methods. Asymptotic analysis then led to operators that had much the same form of the Kirchhoff approximation for forward modeling except for some important distinctions.

The kernels of these inversion formulas all contained a phase function that was of the opposite sign of the phase function in the kernel of the respective forward modeling formula. An important difference between forward modeling formulas and their respective inversion formulas resulted from the distinction that was made between the input variables, $(\boldsymbol{\xi}, \omega)$, and the output variables, \mathbf{y} . The phases of the inversion kernels in the simpler problems have been functions of both the input and output variables. Following this example, our inversion operators should include a phase functions of the form, $-i\omega\tau(\mathbf{y}, \boldsymbol{\xi})$. This is *matched filtering*.

The amplitude of the inversion kernel could also be a function of the input variables $(\boldsymbol{\xi}, \omega)$ and the output variables, \mathbf{y} . The ω dependence of the inversion kernels for reflectivity function β was always a multiplication by a factor of $i\omega$. We will assume that the new inversion formulas for β that we are creating here will have the same dependence, and verify that this assumption is correct later.

Combining these ideas, we conclude that the inversion operator should have the form,

$$\beta(\mathbf{y}) = \int i\omega d\omega \int d^2\xi B(\mathbf{y}, \boldsymbol{\xi}) e^{-i\omega\tau(\mathbf{y}, \boldsymbol{\xi})} u_S(\mathbf{x}_g, \mathbf{x}_s, \omega), \quad (16)$$

where the kernel $B(\mathbf{y}, \boldsymbol{\xi})$ is to be determined.

There are three approaches to the solution of this problem; see Cohen and Hagin [1985], Sullivan and Cohen [1987] and Beylkin [1985]. All three methods lead to the same inversion formula for $\beta(\mathbf{y})$. The method developed here is a synthesis of these three approaches. Only the leading order inversion operator is of interest because we have already restricted the problem to leading order asymptotics in our approximations above. We substitute the data given in (15) into (16), to obtain the cascade of the forward modeling formula and the respective inversion formula

$$\beta(\mathbf{y}) = \int \omega^2 F(\omega) d\omega \int d^2\xi B(\mathbf{y}, \boldsymbol{\xi}) \int d^3x e^{i\omega\{\tau(\mathbf{x}, \boldsymbol{\xi}) - \tau(\mathbf{y}, \boldsymbol{\xi})\}} C(\mathbf{x}, \boldsymbol{\xi}) \beta(\mathbf{x}), \quad (17)$$

where

$$C(\mathbf{x}, \boldsymbol{\xi}) \equiv a(\mathbf{x}, \boldsymbol{\xi}) |\nabla_{\mathbf{x}} \tau(\mathbf{x}, \boldsymbol{\xi})| \quad (18)$$

Let us think of this sixfold integral as a threefold integral in \mathbf{x} of $\beta(\mathbf{x})$ times some kernel function, yielding $\beta(\mathbf{y})$. If this is to be true then the kernel function must, in some asymptotic sense, have the same sifting property as the Dirac delta function, $\delta(\mathbf{y} - \mathbf{x})$ in the integral,

$$\beta(\mathbf{y}) \sim \int d^3x \delta(\mathbf{x} - \mathbf{y}) \beta(\mathbf{x}),$$

or

$$\delta(\mathbf{x} - \mathbf{y}) \sim \int \omega^2 F(\omega) d\omega \int d^2\xi B(\mathbf{y}, \boldsymbol{\xi}) e^{i\omega\{\tau(\mathbf{x}, \boldsymbol{\xi}) - \tau(\mathbf{y}, \boldsymbol{\xi})\}} C(\mathbf{x}, \boldsymbol{\xi}). \quad (19)$$

To understand why this might be so, we must remember that the integral in (17) or (19) is to be evaluated in a high-frequency asymptotic limit, where one might suspect that $\mathbf{x} = \mathbf{y}$ is a dominant critical point of the integrand. We note that the

complex exponential part of the integrand above is an oscillatory function, whose phase is identically zero for $\mathbf{x} = \mathbf{y}$, lending plausibility to the dominant critical point idea. Intuitively, we might expect that the $\boldsymbol{\xi}$ integration would yield a larger result when the oscillations of the phase function are absent—that is, when $\mathbf{x} = \mathbf{y}$ —as compared to the value of the $\boldsymbol{\xi}$ integration when $\mathbf{x} \neq \mathbf{y}$. Therefore, we are interested in approximating this integral for \mathbf{x} in a neighborhood of \mathbf{y} .

Formally, in (19), we may expand the amplitude function $C(\mathbf{x}, \boldsymbol{\xi})$ and the phase function $i\omega \{\tau(\mathbf{x}, \boldsymbol{\xi}) - \tau(\mathbf{y}, \boldsymbol{\xi})\}$ into Taylor's series about the point $\mathbf{x} \equiv \mathbf{y}$. Approximating the amplitude function by the first term of its Taylor's series, we have

$$C(\mathbf{x}, \boldsymbol{\xi}) \approx C(\mathbf{y}, \boldsymbol{\xi}),$$

while the difference in the phase has the approximation,

$$\tau(\mathbf{x}, \boldsymbol{\xi}) - \tau(\mathbf{y}, \boldsymbol{\xi}) \approx \left. \nabla_{\mathbf{x}} \tau(\mathbf{x}, \boldsymbol{\xi}) \right|_{\mathbf{x}=\mathbf{y}} \cdot (\mathbf{x} - \mathbf{y}) + \dots,$$

yields the following:

$$i\omega \{\tau(\mathbf{x}, \boldsymbol{\xi}) - \tau(\mathbf{y}, \boldsymbol{\xi})\} \approx i\mathbf{k} \cdot (\mathbf{x} - \mathbf{y}). \quad (20)$$

Here, $\omega \nabla \tau$ is interpreted as a wave vector \mathbf{k} , through the identity,¹

$$\mathbf{k} \equiv \omega \nabla_{\mathbf{y}} \tau(\mathbf{y}, \boldsymbol{\xi}) \equiv \omega \nabla_{\mathbf{x}} \tau(\mathbf{x}, \boldsymbol{\xi}) \Big|_{\mathbf{x}=\mathbf{y}}. \quad (21)$$

We have approximated the total phase function by the first nonvanishing term of its Taylor's series. This equation defines a change of variable of integration from $(\omega, \boldsymbol{\xi})$ to \mathbf{k} . In terms of the new variables of integration, (19) becomes

$$\delta(\mathbf{x} - \mathbf{y}) \sim \int d^3k \omega^2(\mathbf{k}) F(\omega(\mathbf{k})) \frac{B(\mathbf{y}, \boldsymbol{\xi})}{C(\mathbf{y}, \boldsymbol{\xi})} \left| \frac{\partial(\omega, \boldsymbol{\xi})}{\partial(\mathbf{k})} \right| e^{i\mathbf{k} \cdot (\mathbf{x} - \mathbf{y})}. \quad (22)$$

The function $\omega(\mathbf{k})$ is defined via the expression (21) formally as

$$\omega(\mathbf{k}) = \frac{\mathbf{k} \cdot \nabla_{\mathbf{y}} \tau(\mathbf{y}, \boldsymbol{\xi})}{|\nabla_{\mathbf{y}} \tau(\mathbf{y}, \boldsymbol{\xi})|^2}. \quad (23)$$

It is easier to calculate the reciprocal of the Jacobian appearing in equation (22), that is, the function, $\partial(\mathbf{k})/\partial(\omega, \boldsymbol{\xi})$. To do so, it is sufficient to compute the necessary

¹For \mathbf{y} “near enough” to \mathbf{x} , there exists an exact change of variables from $\omega, \boldsymbol{\xi}$ to \mathbf{k} for which equation (20) is exact, (21) is the leading term of the Taylor series for \mathbf{k} , and (24) is the Jacobian of the change of variables at $\mathbf{x} = \mathbf{y}$.

derivatives directly from the definition of \mathbf{k} in (21). That result is

$$\frac{\partial(\mathbf{k})}{\partial(\omega, \boldsymbol{\xi})} = \omega^2 h(\mathbf{y}, \boldsymbol{\xi}) \quad (24)$$

$$h(\mathbf{y}, \boldsymbol{\xi}) = \det \begin{bmatrix} \nabla_{\mathbf{y}} \tau(\mathbf{y}, \boldsymbol{\xi}) \\ \frac{\partial}{\partial \xi_1} \nabla_{\mathbf{y}} \tau(\mathbf{y}, \boldsymbol{\xi}) \\ \frac{\partial}{\partial \xi_2} \nabla_{\mathbf{y}} \tau(\mathbf{y}, \boldsymbol{\xi}) \end{bmatrix},$$

so that $\partial(\omega, \boldsymbol{\xi})/\partial(\mathbf{k})$ is seen to be a function of \mathbf{y} and $\boldsymbol{\xi}$, only. The right side of (22) is seen to have the form of a forward and inverse Fourier transform with two exceptions. First, note from (22) that $\boldsymbol{\xi}$ is a function of the two independent variables in $\hat{\mathbf{k}} = \mathbf{k}/k$, because

$$\hat{\mathbf{k}} = \text{sgn}(\omega) \nabla_{\mathbf{y}} \tau(\mathbf{y}, \boldsymbol{\xi}) / |\nabla_{\mathbf{y}} \tau(\mathbf{y}, \boldsymbol{\xi})|,$$

relates these variables independent of the choice of $|\omega|$. Thus, the function $a(\mathbf{y}, \boldsymbol{\xi})$, written in the new variables, depends on both $\hat{\mathbf{k}} = \mathbf{k}/k$ and \mathbf{x} . Second, the amplitude of the integrand depends on \mathbf{y} , as well.² Furthermore, if $F(\omega)$ were not identically equal to unity, this could not be an exact inverse transform. Thus, we should expect that, at best, this integral will be an *asymptotic* forward an inverse transform. So, let us pose the problem more mildly; we only ask that $F(\omega) = 1$, the entire integrand should reduce to $1/[2\pi]^3$. That is,

$$\frac{B(\mathbf{y}, \boldsymbol{\xi})}{|h(\mathbf{y}, \boldsymbol{\xi})|C(\mathbf{y}, \boldsymbol{\xi})} = \frac{1}{8\pi^3}, \quad \text{implying that} \quad B(\mathbf{y}, \boldsymbol{\xi}) = \frac{1}{8\pi^3} \frac{|h(\mathbf{y}, \boldsymbol{\xi})|}{a(\mathbf{y}, \boldsymbol{\xi})|\nabla_{\mathbf{y}} \tau(\mathbf{y}, \boldsymbol{\xi})|}. \quad (25)$$

With this value in place, (16) provides the high-frequency inversion of the observed data for the wavespeed perturbation as

$$\beta(\mathbf{y}) = \frac{1}{8\pi^3} \int d^2\xi \frac{|h(\mathbf{y}, \boldsymbol{\xi})|}{a(\mathbf{y}, \boldsymbol{\xi})|\nabla_{\mathbf{y}} \tau(\mathbf{y}, \boldsymbol{\xi})|} \int i\omega d\omega e^{-i\omega\tau(\mathbf{y}, \boldsymbol{\xi})} u_S(\mathbf{x}_g, \mathbf{x}_s, \omega). \quad (26)$$

Implicit in this inversion is an identification of a Fourier wave vector, \mathbf{k} in (21) as a function of frequency and a gradient vector which depends on the particular source-receiver configuration.

The determinant, $h(\mathbf{y}, \boldsymbol{\xi})$ in (24), must be finite and nonzero for the identification of the cascaded model and inversion integral (17) as an approximate Fourier integral (22). Thus, we could use the value of this matrix to characterize source-receiver configurations as providing invertible data by this formalism at an output point, \mathbf{y} .

²This is exactly the kind of integral considered in [Bleistein, 1988]. A justification of the approximations made here by analyzing this general class of integrals appears in that paper and is repeated in Bleistein, et al. [1998]. Note, here, that for this definition of $\hat{\mathbf{k}}$, positive and negative values of ω pick out vectors in both of the directions, $\pm \nabla_{\mathbf{y}} \tau(\mathbf{y}, \boldsymbol{\xi}) / |\nabla_{\mathbf{y}} \tau(\mathbf{y}, \boldsymbol{\xi})|$, as is exploited in that theory.